
 НОВЫЕ
 МИНЕРАЛЫ

**ARSMIRANDITE, $\text{Na}_{18}\text{Cu}_{12}\text{Fe}^{3+}\text{O}_8(\text{AsO}_4)_8\text{Cl}_5$, AND LEHMANNITE,
 $\text{Na}_{18}\text{Cu}_{12}\text{TiO}_8(\text{AsO}_4)_8\text{FCl}_5$, NEW MINERAL SPECIES FROM FUMAROLE
 EXHALATIONS OF THE TOLBACHIK VOLCANO, KAMCHATKA, RUSSIA**

© 2020 г. I. V. Pekov^{1,*}, S. N. Britvin^{2,3}, V. O. Yapaskurt¹, N. N. Koshlyakova¹,
 Yu. S. Polekhovsky², J. Göttlicher⁴, N. V. Chukanov⁵, M. F. Vigasina¹,
 S. V. Krivovichev^{2,3}, A. G. Turchkova¹, and E. G. Sidorov⁶

¹*Faculty of Geology, Moscow State University, Vorobievy Gory, Moscow, 119991 Russia*

²*Institute of Earth Sciences, Saint Petersburg State University,
 University emb., 7/9, Saint Petersburg, 199034 Russia*

³*Kola Science Center RAS, Fersman st., 14, Apatity, 184209 Russia*

⁴*Karlsruhe Institute of Technology, Institute for Synchrotron Radiation,
 Hermann-von-Helmholtz-Platz 1, D-76344, Eggenstein-Leopoldshafen, Germany*

⁵*Institute of Problems of Chemical Physics RAS, Chernogolovka, Moscow region, 142432 Russia*

⁶*Institute of Volcanology and Seismology, Far Eastern Branch RAS,
 Piip Boulevard, 9, Petropavlovsk-Kamchatsky, 683006 Russia*

*e-mail: igorpekov@mail.ru

Received April 8, 2020; Revised April 8, 2020; Accepted April 16, 2020

Abstract—Two closely related new minerals arsmirandite $\text{Na}_{18}\text{Cu}_{12}\text{Fe}^{3+}\text{O}_8(\text{AsO}_4)_8\text{Cl}_5$ and lemannite $\text{Na}_{18}\text{Cu}_{12}\text{Ti}^{4+}\text{O}_8(\text{AsO}_4)_8\text{FCl}_5$ were discovered in sublimates of the Arsenatnaya fumarole at the Second scoria cone of the Northern Breakthrough of the Great Tolbachik Fissure Eruption, Tolbachik volcano, Kamchatka, Russia. They are associated with one another and with hematite, sanidine, sylvite, halite, tenorite, cassiterite, rutile, and various arsenates and sulfates. Arsmirandite and lemannite are visually indistinguishable and occur as equant crystals up to $20 \times 20 \times 30 \mu\text{m}^3$, typically combined in thin crusts up to $2 \times 3 \text{ cm}$. The minerals are dark greyish green to olive-greenish black and have strong vitreous lustre. $D_{\text{calc}} = 3.715$ (arsmirandite) and 3.676 (lemannite) g cm^{-3} . The empirical formula of arsmirandite is $(\text{Na}_{17.06}\text{K}_{0.51}\text{Pb}_{0.08}\text{Ca}_{0.06})_{\Sigma 17.71}(\text{Cu}_{11.73}\text{Mg}_{0.11}\text{Zn}_{0.08}\text{Mn}_{0.01})_{\Sigma 12.93}(\text{Fe}_{0.92}^{3+}\text{Ti}_{0.10}\text{Al}_{0.02})_{\Sigma 1.04}(\text{As}_{7.91}\text{S}_{0.08}\text{P}_{0.03}\text{Si}_{0.02}\text{V}_{0.01})_{\Sigma 8.05}\text{O}_{40.23}\text{Cl}_{4.77}$. The empirical formula of lemannite is $(\text{Na}_{17.92}\text{K}_{0.18}\text{Ca}_{0.24})_{\Sigma 18.34}(\text{Cu}_{11.59}\text{Fe}_{0.21}^{3+})_{\Sigma 11.80}(\text{Ti}_{0.85}\text{Sn}_{0.11})_{\Sigma 0.96}(\text{As}_{7.74}\text{S}_{0.14}\text{P}_{0.09}\text{Si}_{0.03})_{\Sigma 8}\text{O}_{40.10}\text{F}_{0.75}\text{Cl}_{5.42}$. Both minerals are monoclinic, space group $C2/m$, $Z = 2$. Unit-cell parameters (arsmirandite/lemannite) are: $a = 10.742(2)/10.8236(15)$, $b = 21.019(3)/21.1077(17)$, $c = 11.787(2)/11.8561(11) \text{ \AA}$, $\beta = 117.06(3)/117.195(8)^\circ$, and $V = 2370.0(7)/2409.2(5) \text{ \AA}^3$. The crystal structures of arsmirandite and lemannite were solved by means of single-crystal X-ray diffraction analysis. The minerals have two unique structural features: (1) they contain Fe^{3+} and Ti^{4+} in cubic coordination for arsmirandite and lemannite, respectively; (2) their structures are built up by packing of unusual nanoscale ($\sim 1.5 \text{ nm}$ across) clusters with the composition $\{[\text{MCu}_{12}\text{O}_8](\text{AsO}_4)_8\}$ ($M = \text{Fe}^{3+}$ in arsmirandite and Ti^{4+} in lemannite). Each nanocluster contains (MO_8) cube surrounded by twelve flat squares (CuO_4) linked with eight (AsO_4) tetrahedra. Sodium and halogen atoms are located in between the nanoclusters. The name arsmirandite reflects the presence of arsenic and the unusual crystal structure (from the Latin

mirandus, marvellous). Lehmannite is named in honour of the outstanding German and Russian mineralogist and geologist Johann Gottlob Lehmann (1719–1767).

Keywords: arsmirandite, lehmannite, new mineral, arsenate, crystal structure, nanocluster, polyoxometalate, polyoxocuprate, iron in cubic coordination, titanium in cubic coordination, fumarole, Tolbachik volcano, Kamchatka

DOI: 10.31857/S0869605520030077

INTRODUCTION

Fumarole fields related to the Tolbachik volcano at Kamchatka is a unique natural phenomenon, the present-day world record-holder in both number of new mineral species discovered within one geological object and the general diversity of minerals formed in volcanic fumaroles. Tolbachik fumaroles belong to the oxidizing type and the overwhelming majority of minerals formed here are oxocompounds (oxysalts and oxides) and halides (chlorides and fluorides). One of the most remarkable mineralogical features of the Tolbachik fumarole exhalations is the great diversity of arsenate minerals: more than fifty arsenates are discovered here including forty-two (!) new mineral species. All arsenates in Tolbachik fumaroles crystallized under high temperatures (>350–400 °C) and are hence hydrogen-free. The fumarolic arsenate mineralization was recently reviewed by Pekov et al. (2018). The majority of Tolbachik arsenates are concentrated in the sublimates of the active Arsenatnaya fumarole located at the apical part of the Second scoria cone of the Northern Breakthrough of the Great Tolbachik Fissure Eruption 1975–1976 (GTFE). This scoria cone, located 18 km south of the Ploskiy Tolbachik volcano in the central part of Kamchatka Peninsula (Far-Eastern Region, Russia), is a monogenetic volcano about 300 m high and approximately 0.1 km³ in volume formed in 1975 (Fedotov, Markhinin, 1983). Now, forty-five years after the GTFE, its fumarole fields are still active: numerous gas vents with temperatures up to 490 °C were observed by us in 2012–2018.

In the present paper we characterize two structurally related new minerals from the Arsenatnaya fumarole, arsmirandite $\text{Na}_{18}\text{Cu}_{12}\text{Fe}^{3+}\text{O}_8(\text{AsO}_4)_8\text{Cl}_5$ (Cyrillic: арсмирандит) and lehmannite $\text{Na}_{18}\text{Cu}_{12}\text{TiO}_8(\text{AsO}_4)_8\text{FCl}_5$ (Cyrillic: леманнит). The name arsmirandite reflects the presence of arsenic and the very unusual crystal structure, exceptional for a natural compound (from the Latin *mirandus*, marvellous). Lehmannite is named in honour of the outstanding German and Russian mineralogist and geologist Johann Gottlob Lehmann (1719–1767), Academician of the Royal Prussian Academy of Sciences (1754) and the Imperial Russian Academy of Sciences (1761). Since 1761, he worked in St. Petersburg. J.G. Lehmann is, in particular, the author of the original description of crocoite (“red lead ore”, 1766), the first new mineral species discovered in Russia¹ (Vernadsky, 1911).

Both new minerals and their names have been approved by the IMA Commission on New Minerals, Nomenclature and Classification (arsmirandite: IMA2014–081; lehmannite: IMA2017–057a). The type specimens are deposited in the systematic collection of the Fersman Mineralogical Museum of the Russian Academy of Sciences, Moscow, at the catalogue numbers 94623 (arsmirandite) and 96255 (lehmannite). The preliminary report on arsmirandite and lehmannite, focusing on the unique features of their crystal structures was recently published by Britvin et al. (2020).

¹ The name *lehmannite* was proposed by Brooke and Miller (1852) for crocoite, after its discoverer, but has never been in wide use.

OCCURRENCE AND GENERAL APPEARANCE

The general description of the Arsenatnaya fumarole was given by Pekov et al. (2014a, 2018). Specimens containing both new minerals were collected by us from different areas of Arsenatnaya. First samples were found in 2012, but only in 2014 and 2015 we collected the material that gave crystals suitable for the crystal-structure determination of arsmirandite and lemannite, respectively.

The temperatures measured using a chromel-alumel thermocouple at the time of collecting in pockets with arsmirandite and lemannite were 360–450 °C. It seems that both new minerals were deposited from fumarolic gases at temperatures higher than 450 °C. Arsmirandite and lemannite are constituents of fumarolic incrustations consisting of arsenates, sulfates, oxides, chlorides, and silicates. They are associated with one another and with hematite, sanidine (As-bearing variety), sylvite, halite, tenorite, cassiterite, rutile, pseudobrookite, johillerite, bradaczekite, hatertite, magnesiohatertite, arsenatrotitanite, melanarsite, dmisokolovite, shchurovskyite, pharmazincite, katiarsite, lammerite, lammerite- β , urusovite, alarsite, ericlaxmanite, kozyrevskite, yurmarinite, popovite, tilasite, svabite, durangite, anhydrite, aphthalite, langbeinite, calciolangbeinite, steklite, arcanite, palmierite, dolerophanite, euchlorine, wulffite, alumoklyuchevskite, klyuchevskite, krasheninnikovite, vanthoffite, fluoborate, gahnite (Cu-bearing variety), corundum, and fluorophlogopite.

Arsmirandite and lemannite are visually indistinguishable. Both minerals typically occur as solid or, more commonly, interrupted crusts consisting of well-shaped or coarse crystals (Fig. 1, *a–c*), which overgrow basalt scoria and crusts of As-bearing sanidine, hematite or johillerite. Areas covered by interrupted crusts of the new minerals may reach $2 \times 3 \text{ cm}^2$. The crusts are usually not thicker than 50 μm , rarely up to 0.5 mm thick. Open-work clusters of arsmirandite and lemannite crystals occur in cavities. Separate crystals of both new minerals are typically not larger than 5 μm across but some crystals are up to $20 \times 20 \times 30 \mu\text{m}^3$ in size. Crystals are equant, thick tabular or short prismatic with pyramid-like terminations; they are probably shaped by faces of pinacoids and orthorhombic prisms (symmetry class $2/m$) that typically give the combination looking as a rhombic dodecahedron or cuboctahedron, distorted or almost perfect (Fig. 1, *a, c*); some crystals are more complex in shape. Cyclic interpenetration twins morphologically very similar to the twins well-known for the zeolites of the phillipsite series are common for arsmirandite (Fig. 1, *b*). Epitactic overgrowths of tiny lemannite crystals on much bigger crystals of arsenatrotitanite, an arsenate with the idealized formula $\text{NaTiO}(\text{AsO}_4)$ and a titanite-type structure (Pekov et al., 2019), have been observed (Fig. 1, *d*). Lehmannite also forms open-work pseudomorphs after bunches of board- or sword-shaped crystals of an unidentified mineral. The fine-grained, earthy aggregates, sometimes intimately intergrown with As-bearing sanidine or Na-bearing sylvite, are typical for both new minerals.

PHYSICAL PROPERTIES AND OPTICAL DATA

Arsmirandite and lemannite are dark greyish green with an olive hue to olive-greenish black in separate crystals and green or greyish green to olive-drab in earthy aggregates. The crystals have strong vitreous lustre. Both minerals are megascopically almost opaque but thin sections are translucent, dark green. Streak is greyish green with an olive hue. The minerals are brittle. Cleavage or parting is not observed. The fracture is uneven (observed under the scanning electron microscope). The mean micro-indentation hardness (VHN) of lemannite is 416, range is 339–537 kg mm^{-2} (load 100 g). Mohs' hardness was not measured directly because of the small size of crystals of both minerals, the value estimated for lemannite from the micro-indentation hardness is *ca.* 4%. Density could not be measured because of the small size of crystals and porous character of aggregates. Density values calculated using the empirical formulae are 3.715 and 3.676 g cm^{-3} for arsmirandite and lemannite, respectively.

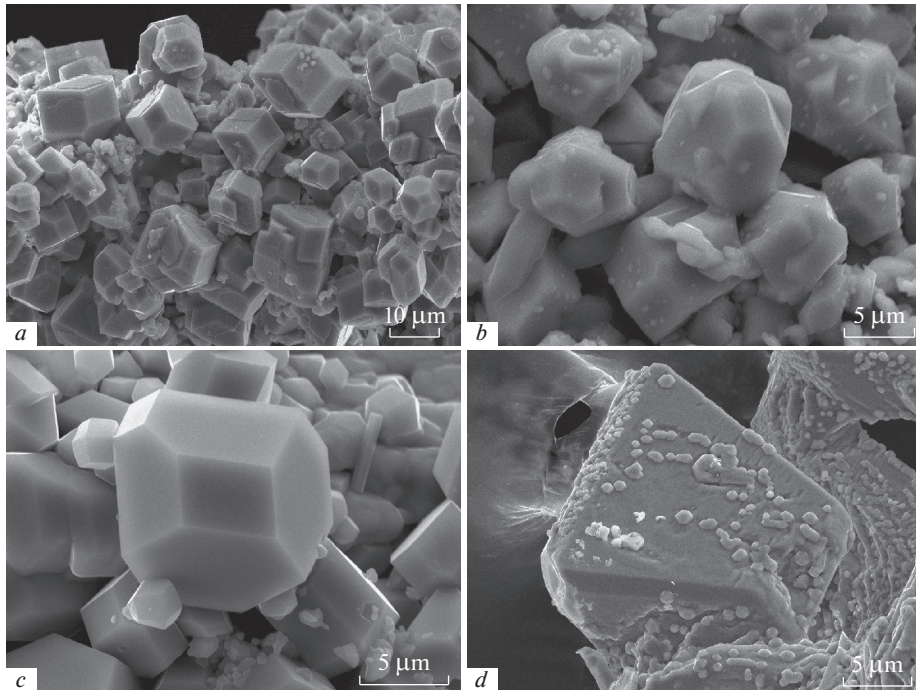


Fig. 1. Morphology of crystals and aggregates of arsmirandite and lehmannite: *a* – crystal crust of arsmirandite, *b* – interpenetration twins of arsmirandite, *c* – lehmannite crystals, *d* – tiny crystals of lehmannite resembling rhombic dodecahedra epitactically overgrowing crystals of arsenatrotitanite. SEM (SE) images.

Рис. 1. Морфология кристаллов и агрегатов арсмирандита и леманнита: *a* – корочка кристаллов арсмирандита, *b* – двойники прорастания арсмирандита, *c* – кристаллы леманнита, *d* – мелкие кристаллы леманнита, по форме напоминающие ромбододекаэдр, эпитаксически нарастают на кристаллы арсенатротитанита. РЭМ-фотографии во вторичных электронах.

Under the microscope in reflected light, both minerals are dark grey, pleochroism was not observed. Bireflectance is very weak, $\Delta R = 0.25\%$ and 0.8% for arsmirandite and lehmannite, respectively (589 nm). Anisotropism is very weak. Weak brown internal reflections were observed for lehmannite. The reflectance values for both minerals measured in air by means of the MSF-21 microspectrophotometer (LOMO, Russia) using the SiC standard (Zeiss, No. 545) are given in Table 1.

RAMAN SPECTROSCOPY

The Raman spectrum of arsmirandite (Fig. 2, *a*) was obtained on a randomly oriented crystal using an EnSpectr R532 instrument (Dept. of Mineralogy, Moscow State University) with a green laser (532 nm) at room temperature. The output power of the laser beam was about 3.5 mW. The spectrum was processed using the EnSpectr expert mode program in the range from 100 to 4000 cm^{-1} with the use of a holographic diffraction grating with 1800 lines per cm and a resolution of 6 cm^{-1} . The diameter of the focal spot on the sample was about 10 μm . The backscattered Raman signal was collected with $40\times$ objective; signal acquisition time for a single scan of the spectral range was 1500 ms and the signal was averaged over 10 scans.

Table 1. Reflectance data of arsmirandite and lemannite**Таблица 1.** Коэффициенты отражения арсмирандита и леманнита

λ , nm	Arsmirandite		Lehmannite		λ , nm	Arsmirandite		Lehmannite	
	R_{\min} , %	R_{\max} , %	R_{\min} , %	R_{\max} , %		R_{\min} , %	R_{\max} , %	R_{\min} , %	R_{\max} , %
400	7.2	7.5	8.3	8.9	560	6.9	7.1	7.9	8.5
420	7.4	7.7	8.2	8.9	580	6.8	7.1	7.8	8.5
440	7.4	7.7	8.2	8.8	589	6.8	7.1	7.6	8.4
460	7.3	7.6	8.1	8.7	600	6.8	7.0	7.7	8.4
470	7.3	7.6	8.1	8.7	620	6.7	7.0	7.7	8.4
480	7.2	7.5	8.1	8.7	640	6.7	7.0	7.6	8.3
500	7.1	7.4	8.0	8.7	650	6.7	7.0	7.6	8.3
520	7.0	7.3	8.0	8.6	660	6.7	6.9	7.6	8.3
540	6.9	7.2	7.9	8.6	680	6.7	6.9	7.5	8.2
546	6.9	7.2	7.9	8.5	700	6.7	6.9	7.5	8.1

The values for wavenumbers (λ) recommended by the IMA Commission on Ore Mineralogy are given in boldtype.

The bands at 823, 846, 866 and 903 cm^{-1} correspond to As^{5+} —O stretching vibrations of AsO_4^{3-} anions. The presence of numerous bands in this region reflects the presence of two non-equivalent, distorted AsO_4 tetrahedra, in line with the structural data (see below). The assignment of the bands in the range from 400 to 700 cm^{-1} is discussed below, in the section Infrared Spectroscopy. Bands with frequencies lower than 400 cm^{-1} correspond to lattice modes involving bending vibrations of AsO_4 tetrahedra and MO_8 polyhedra, as well as Na—Cl stretching vibrations. The absence of bands with frequencies higher than 950 cm^{-1} in the Raman spectrum of arsmirandite indicates the absence of groups with O—H, C—H, C—O, N—H, N—O and B—O bonds.

INFRARED SPECTROSCOPY

Infrared (IR) absorption spectrum of lemannite (Fig. 2, b) was obtained using an ALPHA FTIR spectrometer (Bruker Optics) at a resolution of 4 cm^{-1} and 16 scans. Preliminarily, the sample was powdered, mixed with anhydrous KBr and pelletized. The IR spectrum of an analogous pellet of pure KBr was used as a reference.

The splitting of the bands of As—O stretching vibrations in the range 700–900 cm^{-1} reflects the presence of two nonequivalent distorted AsO_4 tetrahedra in the crystal structure of lemannite. The weak bands at 1112 and 1036 cm^{-1} correspond to asymmetric stretching vibrations of SO_4 and PO_4 tetrahedra that are present in trace amounts in this mineral. The band of banding vibrations of AsO_4 tetrahedra is observed at 371 cm^{-1} .

By analogy with ericlaxmanite and yaroshevskite (Siidra et al., 2020), the bands in the range 430–480 cm^{-1} and at 603 cm^{-1} correspond to Cu—O stretching vibrations in which a major part of energy is concentrated on the long and the shortest Cu—O bonds, respectively. Analogous Raman bands are observed at 472 and 602 cm^{-1} .

According to XANES spectroscopy data (see below), titanium in lemannite is tetravalent. The IR spectrum is in agreement with this conclusion. There is a correlation between the lengths of Ti^{4+} —O bonds and wavenumbers of corresponding stretching vibrations (Chukanov, Chervonnyi, 2016). In particular, stretching vibrations involving four long bonds of the Ti^{4+}O_5

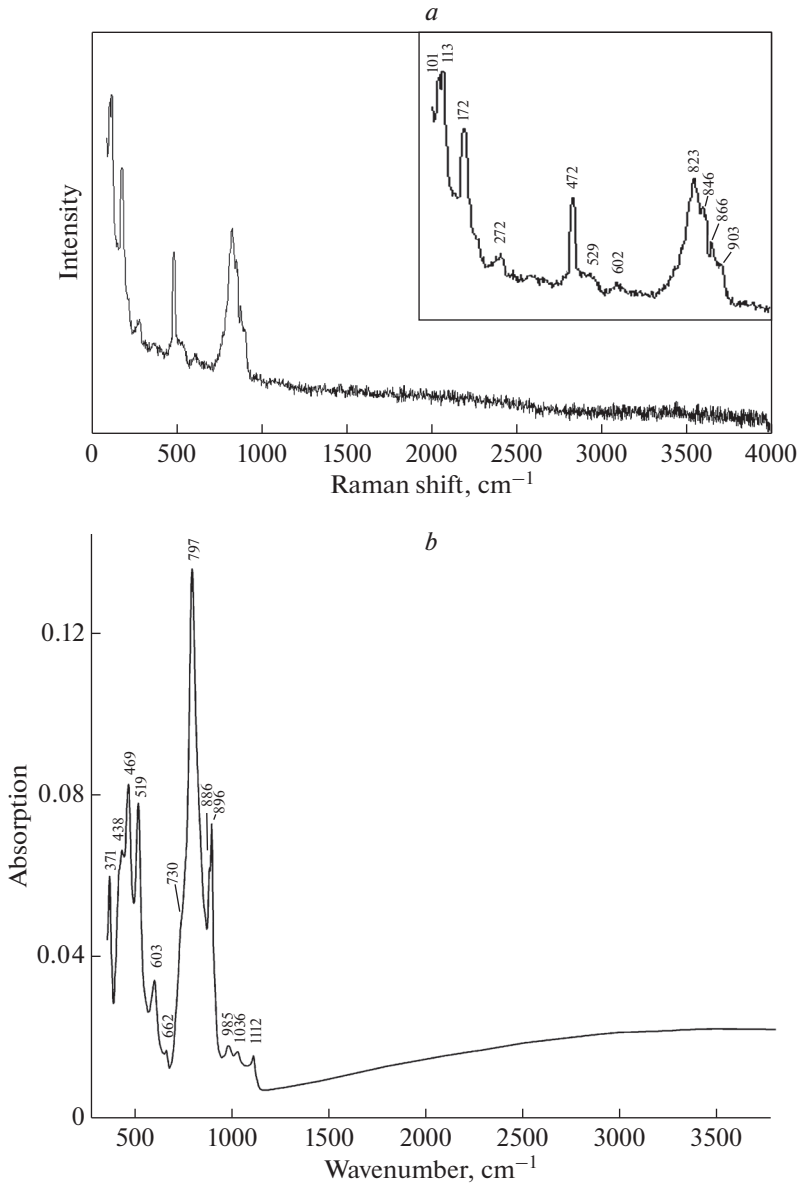


Fig. 2. The Raman spectrum of arsmirandite (*a*) and the IR spectrum of lemannite (*b*).

Рис. 2. КР-спектр арсмирандита (*a*) и ИК-спектр леманнита (*b*).

tetragonal pyramid (lamprophyllite-group minerals, fresnoite, natisite, paranatisite) with the mean Ti–O distances from 1.92 to 2.00 Å are observed in the range 549–627 cm^{-1} whereas the wavenumber of the band related to stretching vibrations of the shortest Ti–O bond of the Ti^{4+}O_5 polyhedron (with the Ti–O distance 1.63–1.69 Å) is about 860 cm^{-1} . The range of Ti–O stretching vibrations of isolated TiO_6 octahedra (in which mean Ti–O distances vary from 1.96 to 2.00 Å) is 540–570 cm^{-1} .

In lemannite, the Ti–O distances are equal to 2.170 and 2.184 Å. Consequently, one should expect a significantly lower frequency of Ti–O stretching vibrations in this mineral. Based on this consideration, the band at 519 cm⁻¹ in the IR spectrum of lemannite is tentatively assigned to Ti–O stretching vibrations. This assumption is in a good agreement with the fact that the analogous Raman band of arsmirandite observed at 529 cm⁻¹ has a very low intensity as compared of the intensity of the band of Cu–O stretching vibrations at 472 cm⁻¹.

The weak IR band at 985 cm⁻¹ may be related to a combination mode of Cu₂–O₈–Ti or Cu₂–O₈–Ti because the sum of wavenumbers of corresponding fundamentals (469 and 519 cm⁻¹) is close to 985 cm⁻¹.

The IR spectrum of lemannite is unique and can be used for its identification. The absence of bands with the frequencies higher than 1120 cm⁻¹ in the IR spectrum of lemannite indicates the absence of groups with O–H, C–H, C–O, N–H, N–O and B–O bonds.

XANES SPECTROSCOPY

A unique cubic coordination of titanium in lemannite and unusually long Ti–O distances (see below) required the direct determination of Ti oxidation state. The latter was carried out using X-ray Absorption Near Edge Structure (XANES) spectroscopy. A sample of lemannite was grinded in an agate mortar and the powder has been glued on a Kapton tape. Spectra have been measured in fluorescence mode at the SUL-X beamline of the ANKA synchrotron ring (Karlsruhe Institute of Technology) on powdered crystals with a focused 27 pole wiggler beam of about 200 μm (hor.) × 100 μm (vert.) at sample position using a Si(111) double crystal monochromator. TiK α fluorescence emission intensities were recorded with a 7 element Si(Li) solid state detector (RAYSPEC, former Gresham) and divided by the incoming signal intensity using an ADC ionization chamber. Ten sample spectra have been measured to achieve good signal-to-noise ratio. Energy step of 0.3 eV has been chosen across the Ti K-edge to resolve spectral features. Spectra were merged and further processed with pre- and post-edge background subtraction and normalization of edge jump of μd 1 using the Athena program of the IFFEFIT software package (Ravel, Newville, 2005).

Ti K XANES spectra of Ti₂O₃ as reference for Ti(III) and two modifications of TiO₂ (rutile and brookite), FeTiO₃ (ilmenite) and CaTiOSiO₄ (titanite) as references for Ti(IV) were measured in transmission using ionization chambers from company ADC. Energy has been calibrated with a Ti foil to 4966 eV (1st maximum of the 1st derivative). As the obtained data show, Ti in lemannite is tetravalent. It is proven by the coincidence of the edge position of the rising flank of the sample Ti K XANES spectrum with a series of the spectra of the above-listed Ti(IV) reference samples (rutile, brookite, titanite, and ilmenite), in contrast to the Ti(III) reference spectrum (Ti₂O₃). The match with the Ti(IV) edge position is shown in Fig. 3 in comparison with the rutile reference spectrum. The edge position of the Ti(IV) reference rutile and of the sample is located at about 3.5 eV above the edge position of the Ti(III) reference (Ti₂O₃) at normalized absorption of μd 0.8 (Fig. 3).

CHEMICAL COMPOSITION

The chemical data for arsmirandite and lemannite were obtained using a Jeol JSM-6480LV scanning electron microscope equipped with an INCA-Wave 500 wavelength-dispersive spectrometer (Laboratory of Analytical Techniques of High Spatial Resolution, Dept. of Petrology, Moscow State University), with an acceleration voltage of 20 kV, a beam current of 20 nA, and a 3 μm beam diameter. The chemical composition of both minerals and standards used are given in Table 2. Contents of other elements with atomic numbers higher than carbon are below detection limits.

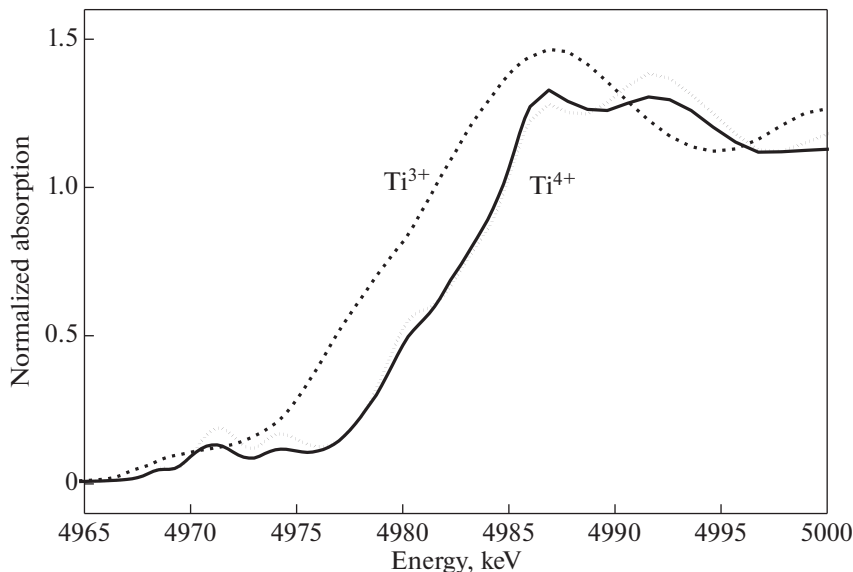


Fig. 3. The Ti *K* XANES spectrum of lehmannite (solid line) compared to the spectra of Ti_2O_3 as reference for Ti(III) (dashed line) and of rutile TiO_2 as reference for Ti(IV) (dotted line).

Рис. 3. Спектр XANES Ti *K* леманнита (сплошная линия) в сравнении с аналогичными спектрами эталонов: Ti_2O_3 для Ti(III) (штриховая линия) и рутила TiO_2 для Ti(IV) (пунктирная линия).

The empirical formula of arsmirandite, calculated on the basis of 45 anions ($\text{O}+\text{Cl}$) *pfu*, is $(\text{Na}_{17.06}\text{K}_{0.51}\text{Pb}_{0.08}\text{Ca}_{0.06})_{\Sigma 17.71}(\text{Cu}_{11.73}\text{Mg}_{0.11}\text{Zn}_{0.08}\text{Mn}_{0.01})_{\Sigma 12.93}(\text{Fe}^{3+}_{0.92}\text{Ti}_{0.10}\text{Al}_{0.02})_{\Sigma 1.04}(\text{As}_{7.91}\text{S}_{0.08}\text{P}_{0.03}\text{Si}_{0.02}\text{V}_{0.01})_{\Sigma 8.05}\text{O}_{40.23}\text{Cl}_{4.77}$. The simplified formula is $\text{Na}_{18}\text{Cu}_{12}\text{Fe}^{3+}\text{O}_8(\text{AsO}_4)_8\text{Cl}_5$, which requires Na_2O 21.06, CuO 36.03, Fe_2O_3 3.01, As_2O_5 34.71, Cl 6.69, $-\text{O}=\text{Cl}$ -1.51, total 100 wt %.

The empirical formula of lehmannite, calculated on the basis of the sum of tetrahedrally coordinated components ($\text{As} + \text{P} + \text{S} + \text{Si}$) = 8 *apfu*, is $(\text{Na}_{17.92}\text{K}_{0.18}\text{Ca}_{0.24})_{\Sigma 18.34}(\text{Cu}_{11.59}\text{Fe}^{3+}_{0.21})_{\Sigma 11.80}(\text{Ti}_{0.85}\text{Sn}_{0.11})_{\Sigma 0.96}(\text{As}_{7.74}\text{S}_{0.14}\text{P}_{0.09}\text{Si}_{0.03})_{\Sigma 8}\text{O}_{40.10}\text{F}_{0.75}\text{Cl}_{5.42}$. The anionic basis of the formula calculation was not used in this case, because of the presence of vacancies at the Cl and F sites (see below). The simplified formula is $\text{Na}_{18}\text{Cu}_{12}\text{Ti}^{4+}\text{O}_8(\text{AsO}_4)_8\text{FCl}_5$, which requires Na_2O 20.97, CuO 35.90, TiO_2 3.00, As_2O_5 34.56, F 0.71, Cl 6.66, $-\text{O}=(\text{F},\text{Cl})$ -1.80, total 100 wt %.

X-RAY CRYSTALLOGRAPHY

Powder X-ray diffraction data of arsmirandite and lehmannite (Tables 3 and 4, respectively) were collected with a Rigaku R-AXIS Rapid II diffractometer equipped with a cylindrical image plate detector (radius 127.4 mm) using Debye-Scherrer geometry, CoK_α radiation (rotating anode with VariMAX microfocus optics), 40 kV, 15 mA and an exposure time of 10 min. Data were integrated using the software package osc2tab (Britvin et al., 2017). Parameters of monoclinic unit cells calculated from the powder data are as follows: arsmirandite: $a = 10.76(2)$, $b = 21.13(1)$, $c = 11.76(2)$ Å, $\beta = 117.0(1)^\circ$ and $V = 2403(5)$ Å 3 ; lehmannite: $a = 10.83(1)$, $b = 21.117(2)$, $c = 11.86(1)$ Å, $\beta = 117.36(7)^\circ$ and $V = 2409(4)$ Å 3 .

Single-crystal X-ray studies of both new minerals were carried out using a Bruker Smart Kappa Apex DUO diffractometer equipped with an APEXII CCD detector. The crystal struc-

Table 2. Chemical composition (wt %) of arsmirandite and lehmannite
Таблица 2. Химический состав (мас. %) арсмирандита и леманнита

Constituent	Arsmirandite			Lehmannite			Probe standard
	mean (5 anal.)	range	SD	mean (8 anal.)	range	SD	
Na_2O	20.04	19.53–20.61	0.43	20.62	19.87–22.91	1.03	Lorenzenite
K_2O	0.91	0.79–1.05	0.10	0.31	0.25–0.36	0.03	Orthoclase
CaO	0.12	0.09–0.16	0.03	0.51	0.09–0.72	0.18	CaWO_4
PbO	0.67	0.59–0.72	0.05	—	—	—	PbTe
MgO	0.17	0.06–0.24	0.07	—	—	—	Diopside
MnO	0.03	0.00–0.06	0.02	—	—	—	Mn
CuO	35.37	34.77–35.89	0.46	34.24	32.75–35.14	0.76	CuFeS_2
ZnO	0.25	0.18–0.36	0.07	—	—	—	ZnS
Al_2O_3	0.03	0.00–0.06	0.02	—	—	—	Al_2O_3
Fe_2O_3	2.79	2.38–3.07	0.27	0.63	0.37–0.88	0.20	CuFeS_2
TiO_2	0.29	0.19–0.40	0.08	2.53	1.96–3.70	0.53	Ilmenite
SnO_2	—	—	—	0.62	0.12–1.37	0.38	SnS
SiO_2	0.05	0.00–0.10	0.04	0.06	0.02–0.10	0.03	Diopside
P_2O_5	0.07	0.05–0.11	0.02	0.23	0.13–0.32	0.06	GaP
V_2O_5	0.04	0.00–0.09	0.03	—	—	—	V
As_2O_5	34.46	34.20–34.75	0.24	33.04	31.84–34.28	0.72	FeAsS
SO_3	0.25	0.17–0.37	0.09	0.43	0.00–2.67	0.43	ZnS
F	—	—	—	0.53	0.48–0.60	0.05	MgF_2
Cl	6.41	6.21–6.49	0.11	7.13	6.94–7.58	0.19	NaCl
$-\text{O}=(\text{F},\text{Cl})$	−1.45	—	—	−1.83	—	—	—
Total	100.50	—	—	99.05	—	—	—

SD – standard deviation; dash means that the content of a constituent is below detection limit.

tures of arsmirandite and lehmannite were solved by direct methods and refined with the use of SHELX-97 software package (Sheldrick, 2008) to $R = 0.051$ and 0.046 , respectively. The detailed structure information for arsmirandite and lehmannite, including coordinates and displacement parameters of atoms and interatomic bond lengths, was reported by Britvin et al. (2020).

DISCUSSION

Crystal Structure

The crystal structures of arsmirandite and lehmannite have been described in detail by Britvin et al. (2020) as based upon unusual nanoscale (~ 1.5 nm across) clusters with the composition $\{[\text{MCu}_{12}\text{O}_8](\text{AsO}_4)_8\}$ (species-defining $M = \text{Fe}^{3+}$ in arsmirandite and Ti^{4+} in lehmannite) as shown in Fig. 4. The nanocluster contains a basic pseudo-cubic unit represented by a nearly perfect (MO_8) cube (the angular deviations from perfect cube are $\pm 0.07^\circ$ for arsmirandite and $\pm 0.62^\circ$ for lehmannite) surrounded by twelve (CuO_4) planar squares. The (CuO_4) polyhedra are corner-linked to eight (AsO_4) tetrahedra. The Na^+ cations and halogen anions are located in between the nanoclusters.

Table 3. Powder X-ray diffraction data of arsmirandite**Таблица 3.** Результаты расчета порошковой рентгенограммы арсмирандита

I_{obs}	d_{obs}	I_{calc}^*	d_{calc}	$h k l$
79	10.58	57, 64	10.568, 10.565	001, 020
100	8.74	94, 100	8.734, 8.730	110, 11-1
9	7.475	20	7.471	021
7	5.683	1, 1, 1	5.679, 5.676, 5.676	111, 13-1, 11-2
46	5.381	98	5.381	20-1
80	5.288	86, 73	5.284, 5.282	002, 040
1	4.783	1	4.795	22-1
3	4.730	5, 6	4.726, 4.725	022, 041
14	3.868	5, 10, 6, 3	3.869, 3.867, 3.867, 3.867	112, 150, 11-3, 15-1
33	3.770	18, 31, 18	3.771, 3.769, 3.769	201, 24-1, 20-3
19	3.737	26	3.736	042
16	3.550	8, 11, 7, 9	3.552, 3.551, 3.550, 3.549	221, 240, 24-2, 22-3
22	3.525	24, 30	2.523, 2.522	003, 060
4	3.435	4, 3, 1, 4	3.435, 3.434, 3.434, 3.434	132, 151, 13-3, 15-2
11	3.343	13, 16	3.342, 3.341	023, 061
27	3.161	20, 18, 20, 20	3.162, 3.161, 3.160, 3.160	310, 33-1, 33-2, 31-3
14	2.946	9, 22, 9	2.948, 2.946, 2.946	202, 26-1, 20-4
15	2.932	15, 22	2.931, 2.930	043, 062
9	2.914	9, 9	2.912, 2.910	330, 33-3
8	2.882	3, 9, 3, 5, 4, 2	2.880, 2.880, 2.879, 2.879, 2.879, 2.879	113, 152, 11-4, 170, 15-3, 17-1
28	2.693	76, 6, 4, 4, 4	2.690, 2.688, 2.687, 2.687, 2.687	40-2, 133, 171, 13-4, 17-2
30	2.643	54, 58	2.642, 2.641	004, 080
4	2.609	1, 2, 1	2.608, 2.607, 2.607	40-1, 42-2, 40-3
74	2.574	64, 69, 68, 77	2.574, 2.574, 2.573, 2.573	242, 261, 24-4, 26-3
18	2.551	16, 14, 13, 18	2.550, 2.550, 2.550, 2.550	331, 350, 35-3, 33-4
2	2.397	2, 4, 2	2.398, 2.397, 2.397	400, 44-2, 40-4
3	2.367	2, 5, 2, 4, 5	2.372, 2.371, 2.363, 2.362	203, 28-1, 20-5, 044, 082
5	2.315	1, 1, 1, 2	2.315, 2.314, 2.313, 2.313	223, 280, 22-5, 28-2
18	2.297	33, 36	2.297, 2.296	351, 35-4
9	2.281	5, 5, 4, 6	2.281, 2.281, 2.280, 2.280	114, 11-5, 190, 19-1
7	2.261	6, 7	2.261, 2.260	262, 26-4
3	2.183	5, 4	2.184, 2.183	440, 44-4
3	2.164	2, 1, 1, 2	2.164, 2.163, 2.163, 2.163	243, 281, 24-5, 28-3
3	2.074	3, 3	2.072, 2.072	025, 0.10.1
3	2.049	3, 3, 3, 3	2.049, 2.049, 2.048, 2.048	51-1, 53-2, 53-3, 51-4
6	1.975	5, 5	1.976, 1.975	53-1, 53-4
3	1.967	4, 1, 4, 7, 1, 1	1.968, 1.967, 1.967, 1.967, 1.967, 1.967	204, 282, 20-6, 2.10.-1, 26-5, 28-4
24	1.885	29, 58, 28, 1	1.886, 1.885, 1.884, 1.884	402, 48-2, 40-6, 115
12	1.868	48	1.868	084
11	1.850	2, 1, 1, 2	1.851, 1.851, 1.850, 1.850	530, 55-1, 55-4, 53-5
2	1.812	2, 2	1.812, 1.812	065, 0.10.3

Table 3. (Contd.)

I_{obs}	d_{obs}	I_{calc}^*	d_{calc}	$h k l$
3	1.775	2, 1, 2, 1	1.776, 1.775, 1.775, 1.775	442, 480, 48-4, 44-6
2	1.765	2, 3	1.765, 1.764	283, 28-5
5	1.642	2, 2, 2, 2, 4, 5	1.642, 1.642, 1.641, 1.641, 1.641, 1.641	423, 4.10.-1, 4.10-3, 42-7, 194, 19-5
10	1.583	11, 11, 11, 11	1.583, 1.582, 1.582, 1.582	512, 59-2, 59-3, 51-7
7	1.533	6, 8, 5, 4, 5, 6	1.535, 1.534, 1.530, 1.530, 1.529, 1.529	482, 48-6, 640, 66-1, 66-5, 64-6
7	1.513	4, 4, 3, 4, 3, 4, 3	1.516, 1.515, 1.512, 1.512, 1.512, 1.511, 1.510	571, 57-6, 265, 2.12.2, 26-7, 2.12.-4, 007
8	1.496	2, 2, 2, 2, 23	1.498, 1.498, 1.498, 1.498, 1.494	71-2, 73-3, 73-4, 71-5, 0.10.5
4	1.477	2, 2, 2, 2	1.477, 1.477, 1.477, 1.477	374, 3.11.2, 37-7, 3.11-5
5	1.469	4, 4	1.469, 1.469	73-2, 73-5
5	1.431	5, 5, 5, 5	1.431, 1.430, 1.430, 1.430	513, 5.11-2, 5.11.-3, 51-8
5	1.416	6, 5, 5, 5	1.416, 1.415, 1.415, 1.415	73-1, 75-2, 75-5, 73-6
16	1.402	21, 20, 21, 18	1.402, 1.401, 1.401, 1.401	246, 24-8, 2.14.1, 2.14.-3
4	1.367	6, 1, 5	1.367, 1.367, 1.367	75-1, 60-8, 75-6
4	1.345	4, 2, 2, 2, 1	1.345, 1.345, 1.345, 1.345, 1.344	80-4, 730, 77-2, 77-5, 73-7

*Only reflections with intensities ≥ 1 are given; the strongest reflections are marked in boldtype.

The most peculiar feature of the discussed structures is the presence of Fe^{3+} (arsmirandite) or Ti^{4+} (lemannite) in a cubic coordination (Fig. 4), which is enforced by the topology of the clusters. The eightfold coordination is untypical for both Fe^{3+} and Ti^{4+} and had so far been unknown for minerals, though reported for several synthetic compounds (Britvin et al., 2020). We note that, for Ti^{4+} , there is an analogy with Zr^{4+} , which shows high (>6) coordination numbers, e.g. in baddeleyite ZrO_2 . The tetravalent state of Ti in lemannite and the trivalent state of Fe in both new minerals is in agreement with the extremely oxidizing conditions of mineral deposition in the Arsenatnaya fumarole (Pekov et al., 2014a, 2018), where the majority of elements demonstrate only their highest oxidation states known in nature: S^{6+} , Mo^{6+} , As^{5+} , V^{5+} , Fe^{3+} , etc.

Description of the crystal structures of arsmirandite and lemannite in terms of anion-centred tetrahedra (Krivovichev et al., 2013) is enlightening. The O8 and O10 atoms do not belong to the arsenate group and are coordinated by three Cu^{2+} and one M (Fe^{3+} or Ti^{4+}) cations each (Fig. 4). As such, OCu_3M tetrahedra linked by sharing common edges constitute the cat-ionic $[\text{O}_8\text{MCu}_{12}]$ core of the $\{\text{MCu}_{12}\text{O}_8\}(\text{AsO}_4)_8$ nanoclusters (Fig. 4). The core is surrounded by eight AsO_4 tetrahedra that are in the face-to-face orientation relative to the OCu_3M tetrahedra (Fig. 4). The metal-oxide $[\text{O}_8\text{MCu}_{12}]$ core of the nanocluster can be considered as a fluorite derivative and as such has been observed in several synthetic compounds (Krivovichev et al., 2013).

As reported by Britvin et al. (2020), the crystal structures of arsmirandite and lemannite can be described as a periodic incorporation of metal-oxide nanoclusters into NaCl matrix, which explains a pseudo-tetragonal symmetry of both minerals (the NaCl matrix is tetragonally compressed). The transformation matrix from true monoclinic ($C2/m$) to pseudo-tetragonal ($I4/mmm$) setting is $(-1/2 -1/2 -1)$ $(-1/2 -1/2 -1)$ $(1\ 0\ 0)$. The lattice parameters of pseudo-tetragonal cell for arsmirandite are: $a = 14.854$ and $c = 10.742$ Å. The relationships between the monoclinic and pseudo-tetragonal unit cells are very similar to those known for the aluminosilicate zeolites of the phillipsite series (Steinfink, 1962; Rinaldi et al., 1974). This

Table 4. Powder X-ray diffraction data of lehmannite

Таблица 4. Результаты расчета порошковой рентгенограммы леманнита

I_{obs}	d_{obs}	I_{calc}^*	d_{calc}	$h k l$
65	10.52	62, 63	10.553, 10.545	020, 001
100	8.74	99, 100	8.763, 8.759	11-1, 110
11	7.44	26	7.460	021
4	5.644	0.5, 0.5, 0.5, 0.5	5.682, 5.681, 5.680, 5.680	13-1, 130, 11-2, 111
36	5.419	95	5.412	20-1
74	5.273	76, 77	5.277, 5.272	040, 002
1	4.826	0.5, 1, 0.5	4.816, 4.816, 4.814	20-2, 22-1, 200
2	4.708	2, 2	4.719, 4.717	041, 022
3	4.382	2, 2	4.381, 4.380	22-2, 220
10	3.861	6, 6, 6, 5	3.866, 3.866, 3.865, 3.863	15-1, 150, 11-3, 112
37	3.772	33, 16, 17	3.778, 3.778, 3.775	24-1, 20-3, 201
13	3.726	33	3.730	042
13	3.552	7, 7, 7, 7	3.557, 3.557, 3.556, 3.555	24-2, 22-3, 240, 221
21	3.511	24, 24	3.518, 3.515	060, 003
4	3.430	2, 2, 2, 2	3.433, 3.432, 3.432, 3.431	15-2, 151, 13-3, 132
11	3.331	12, 13	3.337, 3.335	061, 023
28	3.178	32, 16, 16	3.174, 3.174, 3.173	31-3, 33-1, 310
5	3.071	2, 2	3.072, 3.070	24-3, 241
20	2.947	18, 9, 9	2.950, 2.949, 2.947	26-1, 20-4, 202
24	2.927	18, 18, 12, 12	2.926, 2.926, 2.921, 2.920	062, 043, 33-3, 330
11	2.876	2, 2, 6, 6, 3, 2	2.878, 2.878, 2.877, 2.876, 2.876, 2.875	17-1, 170, 15-3, 152, 11-4, 113
22	2.712	72	2.706	40-2
18	2.687	5, 5, 5, 5	2.685, 2.684, 2.684, 2.683	17-2, 171, 13-4, 133
43	2.636	55, 57	2.638, 2.636	080, 004
98	2.573	68, 69, 68, 70	2.575, 2.574, 2.574, 2.573	26-3, 24-4, 261, 242
32	2.553	19, 19, 19, 19	2.556, 2.555, 2.555, 2.554	35-3, 33-4, 350, 331
5	2.373	4, 2, 2	2.372, 2.371, 2.370	28-1, 20-5, 203
3	2.358	4, 4	2.360, 2.358	082, 044
30	2.301	38	2.300	35-4
5	2.277	5, 5, 5, 5	2.279, 2.279, 2.277, 2.277	19-1, 190, 11-5, 114
5	2.260	8, 8	2.260, 2.259	26-4, 262
4	2.201	5, 5	2.191, 2.190	44-4, 440
2	2.162	1, 1, 1, 1	2.163, 2.163, 2.162, 2.162	28-3, 281, 24-5, 243
1	2.144	0.5, 0.5	2.142, 2.142	51-3, 51-2
6	2.068	4, 5	2.070, 2.068	0.10.1, 025
4	1.981	5, 5	1.985, 1.985	53-4, 53-1
8	1.965	7, 4, 4	1.966, 1.966, 1.965	2.10.-1, 20-6, 204
33	1.889	56, 28, 28	1.889, 1.889, 1.888	48-2, 40-6, 402
15	1.864	55	1.865	084
11	1.842	6, 7, 7, 7	1.843, 1.842, 1.842, 1.841	2.10.-3, 2.10.1, 24-6, 244

Table 4. (Contd.)

I_{obs}	d_{obs}	I_{calc}^*	d_{calc}	$h k l$
4	1.779	2, 2, 2, 2	1.779, 1.778, 1.778, 1.777	48-4, 44-6, 62-3, 442
2	1.762	3, 3	1.763, 1.763	28-5, 283
3	1.646	1, 1, 0.5, 0.5, 0.5, 0.5	1.648, 1.647, 1.647, 1.647, 1.646, 1.646	0.10.4, 085, 39-5, 37-6, 392, 373
2	1.623	2, 2	1.624, 1.624	64-5, 641
12	1.586	13, 25, 0.5, 12	1.586, 1.586, 1.586, 1.585	59-3, 59-2, 443, 512
6	1.540	7, 11, 6, 7, 6	1.536, 1.536, 1.535, 1.535, 1.535	48-6, 66-5, 66-1, 482, 640
4	1.510	4, 4, 4, 4	1.511, 1.510, 1.510, 1.510	2.12.-4, 2.12.2, 26-7, 265
7	1.491	1, 32, 1	1.493, 1.492, 1.491	0.14.1, 0.10.5, 027
2	1.478	2, 4, 2, 2, 4, 2	1.477, 1.477, 1.477, 1.477, 1.476, 1.475	3.11.-5, 73-5, 37-7, 3.11.2, 73-2, 374
4	1.451	5, 2, 2, 5, 2, 2, 5	1.452, 1.452, 1.451, 1.450, 1.449, 1.449, 1.449	2.14.-1, 20-8, 206, 0.14.2, 3.13.-3, 3.13.0, 047
11	1.435	3, 3, 1, 1	1.438, 1.438, 1.438, 1.438	2.10.-6, 2.10.4, 22-8, 226
6	1.407	2, 0.5, 0.5, 2, 2, 0.5, 0.5, 2	1.407, 1.407, 1.407, 1.407, 1.407, 1.406, 1.406, 1.406	5.11.-4, 59-6, 57-7, 5.11.-1, 53-8, 591, 572, 533
18	1.401	26, 26, 27, 27	1.400, 1.400, 1.400, 1.399	2.14.-3, 2.14.1, 24-8, 246
2	1.377	6, 6	1.373, 1.373	75-6, 75-1
2	1.351	4, 0.5, 0.5, 1, 1, 2, 2	1.353, 1.351, 1.351, 1.350, 1.350, 1.350, 1.350	80-4, 0.12.5, 0.10.6, 73-7, 77-5, 77-2, 730

* Only reflections with $I_{\text{calc}} \geq 0.5$ are given; the strongest reflections are marked in boldtype.

similarity, albeit solely geometric, may explain the similarity of pseudo-tetragonal twins of arsmirandite (Fig. 1, b) to the well-known twins of the phillipsite-group minerals.

Relationship of arsmirandite and lemannite to one another and with other minerals

The difference between arsmirandite and lemannite is related to the nature of the M cation. Since Fe^{3+} and Ti^{4+} possess different charges, substitution of trivalent iron for tetravalent titanium requires corresponding compensation of the charge balance as described by Britvin et al. (2020). The main formal substitution scheme responsible for the transition from arsmirandite to lemannite is: $\text{Fe}^{3+} + \square^0 \rightarrow \text{Ti}^{4+} + \text{F}^-$. Thus, the idealized, end-member formula of lemannite contains 46 anions instead of 45 in arsmirandite (Table 5).

The topology of the metal-oxide-arsenate clusters in the two minerals is similar to that observed in polyoxopalladates [see Britvin et al. (2020) for references]. Lehmannite is the third natural hydrogen-free arsenate with the species-defining Ti, after katiarsite, $\text{KTiO}(\text{AsO}_4)$ (Pekov et al., 2016), and arsenatrotitanite, $\text{NaTiO}(\text{AsO}_4)$ (Pekov et al., 2019). All three minerals were found in high-temperature sublimes in the same Arsenatnaya fumarole. Braithwaiteite, ideally $\text{NaCu}_5(\text{Ti}^{4+}\text{Sb}^{5+})\text{O}_2(\text{AsO}_4)_4[\text{AsO}_3(\text{OH})]_2 \cdot 8\text{H}_2\text{O}$, demonstrates some similarity to lemannite in terms of the chemical composition, but it is a highly hydrated arsenate formed in oxidation zone of a sulfide copper deposit (Paar et al., 2009).

From the chemical point of view, both arsmirandite and lemannite are polyoxocuprates and belong to the emerging class of minerals containing polyoxometalate clusters (Krivovichev, 2020). As a rule, polyoxometalate minerals crystallize from low-temperature aqueous environments, mostly in oxidation zones of mineral deposits. For instance, bouazzerite,

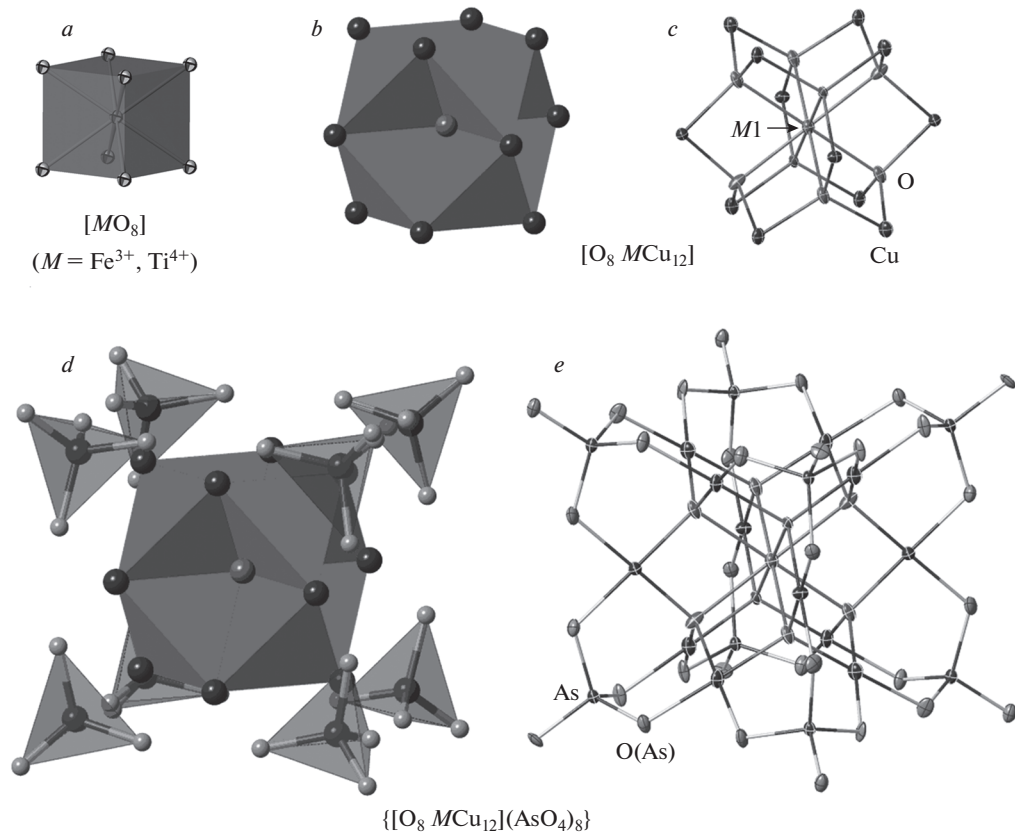


Fig. 4. The structure of the arsenate nanoclusters in arsmirandite and lehmannite shown in ellipsoidal and polyhedral representations (exemplified by arsmirandite): *a* – cubic coordination of *M1* site; *b, c* – 13-nuclear metal-oxide core; *d, e* – the whole clusters. Displacement ellipsoids are shown at the 50% probability level.

Рис. 4. Строение арсенатных нанокластеров в арсмирандите и леманните, показанное на примере арсмирандита с помощью эллипсоидов (*c, e*) и в полиэдрическом представлении (*a, b, d*): *a* – кубическая координация позиции *M1*; *b, c* – 13-ядерная оксидная центральная часть кластера; *d, e* – кластер целиком.

$Bi_6(Mg,Co)_{11}Fe_{14}(AsO_4)_{18}O_{12}(OH)_4(H_2O)_{86}$ (Brugger et al., 2007), and whitecapsite, $H_{16}Sb_6^{3+}Fe_5^{2+}Fe_{14}^{3+}(AsO_4)_{18}O_{16}(H_2O)_{120}$ (Pekov et al., 2014b), which are both based upon heptanuclear metal-oxide core arsenate nanoclusters, have been discovered in oxidation zones, where they crystallized from low-temperature solutions. In contrast, arsmirandite and lehmannite are the first and the only known minerals that contain polyoxometalate clusters and form in anhydrous high-temperature fumarolic environments.

ACKNOWLEDGEMENTS

This study was supported by the Russian Science Foundation, grant No. 19-17-00050 in parts of mineralogical studies, determination of chemical composition of both new minerals and Raman spectroscopy of arsmirandite. IR spectroscopic measurements for lehmannite have been carried out in accordance with the state task, state registration No. 0089-2019-0013. The technical support by the SPbSU X-Ray Diffraction Resource Center and Centre for Physical Methods of Surface Investigation is acknowledged.

Table 5. Comparative data for arsmirandite and lehmannite***Таблица 5.** Сравнительная характеристика арсмирандита и леманнита*

Mineral	Arsmirandite $\text{Na}_{18}\text{Cu}_{12}\text{Fe}^{3+}\text{O}_8(\text{AsO}_4)_8\text{Cl}_5$	Lehmannite $\text{Na}_{18}\text{Cu}_{12}\text{Ti}^{4+}\text{O}_8(\text{AsO}_4)_8\text{FCl}_5$ Monoclinic $C2/m$
Idealized formula		
Crystal system		Monoclinic
Space group		$C2/m$
$a, \text{\AA}$	10.742 (2)	10.8236 (15)
$b, \text{\AA}$	21.019 (3)	21.1077 (17)
$c, \text{\AA}$	11.787 (2)	11.8561 (11)
$\beta, {}^\circ$	117.06 (3)	117.195 (8)
$V, \text{\AA}^3$	2370.0 (7)	2409.2 (5)
Z	2	2
$D_{\text{calc}}, \text{g cm}^{-3}$	3.715	3.676
Strongest reflections of the powder X-ray diffraction pattern:	10.58 – 79	10.52 – 65
$d, \text{\AA} - I, \%$	8.74 – 100 5.381 – 46 5.288 – 80 3.770 – 33 2.693 – 28 2.643 – 30 2.574 – 74	8.74 – 100 5.419 – 36 5.273 – 74 3.772 – 37 2.636 – 43 2.573 – 98 1.889 – 33

* Unit-cell parameters are from single-crystal X-ray diffraction data (Britvin et al., 2020).

REFERENCES

- Britvin S.N., Dolivo-Dobrovolsky D.V., Krzhizhanovskaya M.G. Software for processing the X-ray powder diffraction data obtained from the curved image plate detector of Rigaku RAXIS Rapid II diffractometer. *Zapiski RMO (Proc. Russian Miner. Soc.)*. **2017**. Vol. 146. N 3. P. 104–107 (in Russian).
- Britvin S.N., Pekov I.V., Yapaskurt V.O., Koshlyakova N.N., Göttlicher J., Krivovichev S.V., Turchkova A.G., Sidorov E.G. Polyoxometalate chemistry at volcanoes: discovery of a novel class of polyoxocuprate nanoclusters in fumarolic minerals. *Sci. Rep.* **2020**. Vol. 10. Paper 6345.
- Brooke H.J., Miller W.H. An Elementary Introduction to Mineralogy by the late William Phillips. New Edition with extensive alterations and additions. Longman, Brown, Green and Longmans, London, 1852.
- Brugger J., Meisser N., Krivovichev S., Armbruster T., Favreau G. Mineralogy and crystal structure of bouazzerite from Bou Azzer, Anti-Atlas, Morocco: Bi-As-Fe nanoclusters containing Fe^{3+} in trigonal prismatic coordination. *Amer. Miner.* **2007**. Vol. 92. P. 1630–1639.
- Chukanov N.V., Chervonnyi A.D. Infrared Spectroscopy of Minerals and Related Compounds. Springer Verlag, Cham, **2016**. 1109 pp.
- Fedotov S.A., Markhinin Y.K., eds. The Great Tolbachik Fissure Eruption. Cambridge University Press, New York, **1983**. 341 pp.
- Krivovichev S.V. Polyoxometalate clusters in minerals: review and complexity analysis. *Acta Crystallogr.* **2020**. Vol. B76 (in press).
- Krivovichev S.V., Mentré O., Siidra O.I., Colmont M., Filatov S.K. Anion-centered tetrahedra in inorganic compounds. *Chem. Rev.* **2013**. Vol. 113. P. 6459–6535.
- Paar W.H., Cooper M.A., Hawthorne F.C., Moffatt E., Gunther M.E., Roberts A.C., Dunn P.J. Braithwaiteite, $\text{NaCu}_5(\text{TiSb})_2\text{O}_7(\text{AsO}_4)[\text{AsO}_3(\text{OH})]_2 \cdot 8\text{H}_2\text{O}$, a new mineral species from Laurani, Bolivia. *Canad. Miner.* **2009**. Vol. 47. P. 947–952.
- Pekov I.V., Zubkova N.V., Yapaskurt V.O., Belakovskiy D.I., Lykova I.S., Vigasina M.F., Sidorov E.G., Pushcharovsky D.Yu. New arsenate minerals from the Arsenatnaya fumarole, Tolbachik volcano, Kamchatka, Russia. I. Yurmarinite, $\text{Na}_7(\text{Fe}^{3+}, \text{Mg}, \text{Cu})_4(\text{AsO}_4)_6$. *Miner. Mag.* **2014a**. Vol. 78. P. 905–917.
- Pekov I.V., Zubkova N.V., Göttlicher J., Yapaskurt V.O., Chukanov N.V., Lykova I.S., Belakovskiy D.I., Jensen, M.C., Leising J.F., Nikischer A.J., Pushcharovsky D.Yu. Whitecapsite, a new hydrous iron and trivalent

antimony arsenate mineral from the White Caps mine, Nevada, USA. *Eur. J. Miner.* **2014**b. Vol. 26. P. 577–587.

Pekov I.V., Yapaskurt V.O., Britvin S.N., Zubkova N.V., Vigasina M.F., Sidorov E.G. New arsenate minerals from the Arsenatnaya fumarole, Tolbachik volcano, Kamchatka, Russia. V. Katarsite, $\text{KTiO}(\text{AsO}_4)$. *Miner. Mag.* **2016**. Vol. 80. P. 639–646.

Pekov I.V., Koshyakova N.N., Zubkova N.V., Lykova I.S., Britvin S.N., Yapaskurt V.O., Agakhanov A.A., Shchipalkina N.V., Turchkova A.G., Sidorov E.G. Fumarolic arsenates – a special type of arsenic mineralization. *Eur. J. Miner.* **2018**. Vol. 30. P. 305–322.

Pekov I.V., Zubkova N.V., Agakhanov A.A., Belakovskiy D.I., Vigasina M.F., Yapaskurt V.O., Sidorov E.G., Britvin S.N., Pushcharovsky D.Yu. New arsenate minerals from the Arsenatnaya fumarole, Tolbachik volcano, Kamchatka, Russia. IX. Arsenatrotitanite, $\text{NaTiO}(\text{AsO}_4)$. *Miner. Mag.* **2019**. Vol. 83. P. 453–458.

Ravel B., Newville M. ATHENA, ARTEMIS, HEPHAESTUS: Data analysis for X-ray absorption spectroscopy using IFEFFIT. *J. Synchr. Rad.* **2005**. Vol. 12. P. 537–541.

Rinaldi R., Pluth J.J., Smith J.V. Zeolites of the phillipsite family. Refinement of the crystal structures of phillipsite and harmotome. *Acta Crystallogr.* **1974**. Vol. B30. P. 2426–2433.

Shannon R.D. Revised effective ionic radii and systematic studies of interatomic distances in halides and chalcogenides. *Acta Crystallogr.* **1976**. Vol. A32. P. 751–767.

Sheldrick G.M. A short history of SHEXL. *Acta Crystallogr.* **2008**. Vol. A64. P. 112–122.

Sidra O.I., Vladimirova V.A., Tsirlin A.A., Chukanov N.V., Ugolkov V.L. $\text{Cu}_9\text{O}_2(\text{VO}_4)_4\text{Cl}_2$, a first copper oxychloride vanadate: mineralogically inspired synthesis and magnetic behaviour. *Inorg. Chem.* **2020**. Vol. 59. P. 2136–2143.

Steinfink H. The crystal structure of the zeolite, phillipsite. *Acta Crystallogr.* **1962**. Vol. 15. P. 644–651.

Vernadsky V.I. On the discovery of crocoite. *Lomonosovskii Sbornik*. Saint Petersburg, **1911**. P. 345–354 (in Russian).

АРСМИРАНДИТ $\text{Na}_{18}\text{Cu}_{12}\text{Fe}^{3+}\text{O}_8(\text{AsO}_4)_8\text{Cl}_5$ И ЛЕМАННИТ $\text{Na}_{18}\text{Cu}_{12}\text{TiO}_8(\text{AsO}_4)_8\text{FCl}_5$ – НОВЫЕ МИНЕРАЛЫ ИЗ ФУМАРОЛЬНЫХ ЭКСТАЛИЯЦИЙ ВУЛКАНА ТОЛБАЧИК (КАМЧАТКА, РОССИЯ)

© 2020 г. д. чл. И. В. Пеков^{a,*}, д. чл. С. Н. Бритвин^{b, c}, В. О. Япаскурт^a, Н. Н. Кошлякова^a, д. чл. Ю. С. Полеховский^b, И. Гёттихер^d, д. чл. Н. В. Чуканов^e, М. Ф. Вигасина^a, д. чл. С. В. Кривовичев^{b, c}, д. чл. А. Г. Турчкова^a, д. чл. Е. Г. Сидоров^f

^aМосковский государственный университет, геологический факультет,
 Воробьевы горы, Москва, 119991 Россия

^bИнститут наук о Земле, Санкт-Петербургский государственный университет,
 Университетская наб., 7/9, Санкт-Петербург, 199034 Россия

^cКольский научный центр РАН, ул. Ферсмана, 14, Апатиты, 184209 Россия

^dТехнологический институт Карлсруэ, Эггенштейн-Леопольдсхафен, Германия

^eИнститут проблем химической физики РАН,
 пр-т Академика Семёнова, д. 1, Черноголовка, Московская обл., 142432 Россия

^fИнститут вулканологии и сейсмологии, ДВО РАН,
 бул. Пийна, 9, Петропавловск-Камчатский, 683000 Россия

*e-mail: igorpekov@mail.ru

Два близкородственных друг другу новых минерала арсмирандит $\text{Na}_{18}\text{Cu}_{12}\text{Fe}^{3+}\text{O}_8(\text{AsO}_4)_8\text{Cl}_5$ и леманнит $\text{Na}_{18}\text{Cu}_{12}\text{Ti}^{4+}\text{O}_8(\text{AsO}_4)_8\text{FCl}_5$ установлены в воззонах фумаролы Арсенатной на Втором шлаковом конусе Северного прорыва Большого трещинного Толбачинского извержения (вулкан Толбачик, Камчатка). Они ассоциируют друг с другом, а также с гематитом, санидином, сильвином, галитом, теноритом, кассiterитом, рутилом, различными арсенатами и сульфатами. Арсмирандит и леманнит визуально неразличимы. Они образуют изометричные кристаллы размером до $20 \times 20 \times 30$ мкм, обычно собранные в тонкие корочки размером до 2×3 см. Оба минерала темные серовато-зеленые до черных с оливково-зеленым оттенком, блеск сильный стеклянный. $D_{\text{вып}} = 3.715$ (арсмирандит) и 3.676 (леманнит) г/см³. Эмпирическая формула арсмирандита $(\text{Na}_{17.06}\text{K}_{0.51}\text{Pb}_{0.08}\text{Ca}_{0.06})_{\Sigma 17.71}(\text{Cu}_{11.73}\text{Mg}_{0.11})$

$\text{Zn}_{0.08}\text{Mn}_{0.01})_{\Sigma 12.93}(\text{Fe}^{3+}_{0.92}\text{Ti}_{0.10}\text{Al}_{0.02})_{\Sigma 1.04}(\text{As}_{7.91}\text{S}_{0.08}\text{P}_{0.03}\text{Si}_{0.02}\text{V}_{0.01})_{\Sigma 8.05}\text{O}_{40.23}\text{Cl}_{4.77}$, леманнита – $(\text{Na}_{17.92}\text{K}_{0.18}\text{Ca}_{0.24})_{\Sigma 18.34}(\text{Cu}_{11.59}\text{Fe}^{3+}_{0.21})_{\Sigma 11.80}(\text{Ti}_{0.85}\text{Sn}_{0.11})_{\Sigma 0.96}(\text{As}_{7.74}\text{S}_{0.14}\text{P}_{0.09}\text{Si}_{0.03})_{\Sigma 8}\text{O}_{40.10}\text{F}_{0.75}\text{Cl}_{5.42}$. Оба минерала моноклинные, пр. гр. $C2/m$, $Z = 2$. Параметры их элементарных ячеек (арсмирандит/леманнит): $a = 10.742(2)/10.8236(15)$, $b = 21.019(3)/21.1077(17)$, $c = 11.787(2)/11.8561(11)$ Å, $\beta = 117.06(3)/117.195(8)^\circ$, $V = 2370.0(7)/2409.2(5)$ Å³. Кристаллические структуры арсмирандита и леманнита определены на монокристаллах. Эта пара минералов обладает двумя уникальными структурными чертами: (1) Fe^{3+} и Ti^{4+} в них находятся в кубической координации; (2) в основе их структур лежат необычные наноразмерные (~ 1.5 нм в поперечнике) кластеры $\{[MCu_{12}\text{O}_8](\text{AsO}_4)_8\}$, где $M = \text{Fe}^{3+}$ в арсмирандите и Ti^{4+} в леманните. Ядро такого нанокластера образует куб (MO_8); он окружен двенадцатью плоскими квадратами (CuO_4), к которым присоединены восемь тетраэдров (AsO_4). Атомы Na и галогенов находятся между нанокластерами. Название арсмирандита отражает присутствие As (*arsenic*) и необычную кристаллическую структуру: *mirandus* – по-латински удивительный. Леманнит назван в честь выдающегося немецко-российского минерала и геолога Иоганна Готтлоба Леманна (1719–1767).

Ключевые слова: арсмирандит, леманнит, новый минерал, арсенат, кристаллическая структура, нанокластер, полиоксометаллат, полиоксокупрат, железо в кубической координации, титан в кубической координации, фумарола, вулкан Толбачик, Камчатка

СПИСОК ЛИТЕРАТУРЫ

Бритвин С.Н., Доливо-Добровольский Д.В., Кржижановская М.Г. Программный пакет для обработки рентгеновских порошковых данных, полученных с цилиндрического детектора дифрактометра Rigaku RAXIS Rapid II // Записки РМО. 2017. Ч. 146. Вып. 3. С. 104–107.

Вернадский В.И. Об открытии крокоита // Ломоносовский сборник. СПб., 1911. С. 345–354.